The energy diagram of NiO within an LCAO-LSDA+ *U* approach

1997 J. Phys.: Condens. Matter 9 647

(http://iopscience.iop.org/0953-8984/9/3/005)

J. Phys.: Condens. Matter **9** (1997) 647–661. Printed in the UK PII: S0953-8984(97)76622-0

The energy diagram of NiO within an LCAO-LSDA + U approach

J Hugel and M Kamal

Laboratoire de Spectrométrie Optique de la Matière, Université de Metz–IPC, 1 Boulevard Arago, 57078 Metz Cédex 3, France

Received 25 July 1996

Abstract. The itinerant LCAO picture based on localized atomic-like orbitals has been used to study the electronic ground state of NiO. The U-corrected local spin-density approximation (LSDA+U) yields energy-dispersion curves which show satisfactory agreement with the angular photoemission measurements. As a result the d states appear as narrow and well identified bands located above the 2p oxygen bands. The on-site Coulomb energy U increases the 2p character within the upper d valence band but not to the extent that NiO can be considered as a charge-transfer insulator.

1. Introduction

It is well known that the classical band theory failed to describe the electronic properties of NiO. The failure has been straightforwardly ascribed to the d electrons. Their small spread in space and their atomic representation in terms of unclosed shells lie at the origin of the problem. The difficulty has given rise to many theoretical and experimental studies but none of the efforts were able to provide a definite answer at the time. NiO is the prototype of the Mott–Hubbard insulators in which the forbidden gap separates the occupied from the empty d bands. The early classification proposed by Mott [1] has evolved towards the concept of a charge-transfer insulator characterized by an upper p-predominant valence band after the spectroscopic data were successfully interpreted within the model of Fujimori and Minami [2]. The wide acceptance of the inverted classical Mott–Hubbard scheme stems from the assignment of the resonant satellite peak in term of pure d^7 states.

Two points of view compete amidst all the theoretical approaches. One concept is that the one-electron scheme is not suitable for describing strongly correlated electronic systems. Mott was the first to notice that the electronic interactions were not properly described in the classical band Hamiltonian. The deficiency has been reduced by Hubbard in his well known Hamiltonian with the introduction of the intrasite electrostatic interactions. The second concept, that of Slater [3], admits the fundamentals of the band theory and imputes the observed difficulties to the lack of realism in the physical description. The merit of Slater's concept lay in his proposal of the spin-polarized approach as a means by which to treat the antiferromagnetic ordering. The first confirmation has been obtained by Terakura *et al* [4]. They explained the appearance of a small forbidden gap in NiO as a crystal-field effect. This result removed the doubt about the band theory and generated fruitful developments.

A well recognized method for describing the ground state in chemistry and in solid-state physics is that of the density functional theory (DFT) of Kohn and Sham [5]. For practical

0953-8984/97/030647+15$19.50

purposes the theory is used within its local density approximation (LDA). In principle the theory treats the exchange energy and the correlation energy on the same level and has furnished satisfactory results for slowly varying densities. Its limitation appeared when the local spin-density approximation (LSDA) was unable to reproduce the electrical behaviour of the transition monoxide series. Since the LSDA was founded on a homogeneous electron density it became obvious that one could ascribe the disagreement to the localized character of the d or f electrons. In order to reduce the discrepancy appearing in the practical application of the Kohn–Sham theory, various corrections have been proposed.

A general correction consists in employing a non-uniform density in order to better account for the exchange–correlation potential. The attempt is based on the gradient expansion with the aim of improving the homogeneous gas results. Various expressions for the exchange–correlation potential have been proposed and have generally been termed the general gradient approximation (GGA).

Recently Dufek *et al* [6] established as a general rule that the GGA [7] reduces the occupied bandwidths and that it emphasizes the band separation. Thus for NiO the band gap increases from 0.4 eV in the absence of correction to 1.2 eV when it is applied. Further Dufek *et al* [8] showed that when another version of the GGA [9] is used, FeO and CoO become insulating. They also indicate in their former work that the angular gradient enhances the asphericity of the exchange–correlation potential and in the case of CoO plays a part in stabilizing the magnetic state. The asphericity acts on the electronic density by destroying the fourfold symmetry. The last theoretical prediction is not actually confirmed by the experiment [10].

A less general way of taking correlation effects into account is given by the self-interaction correction (SIC). Its purpose is to cure the lack of compensation between the self-exchange correlation energy and the self-Coulomb energy. The correction systematically lowers the occupied states since it consists in subtracting the potential created by the charge density on itself. Svane and Gunnarsson [11] on one hand and Szotek *et al* [12] on the other observed that the action of the SIC leads to a reversal of the d bands with respect to the oxygen 2p bands because the most significant correction occurs for the localized d electrons. The forbidden band of NiO is 2.54 eV wide and shows appreciable progress over the non-corrected LSDA.

Another way of introducing the correlation effects has been proposed by Anisimov *et al* [13]. Their idea is to reduce the drawbacks resulting from the use of a local spherical density by taking into account the fluctuations of the orbital occupation numbers. The discrepancies become significant for atoms having a non-filled shell whereas they are practically missing for a saturated shell. In the LDA, as in the Hartree–Fock approaches, these fluctuations are generally neglected although they are embedded in these methods as soon as a spherical density is considered. In order to re-establish the right occupation number Anisimov *et al* [13] introduced an orbital-dependent potential into the LDA scheme. This potential depends upon two parameters, the Coulomb interaction U and the exchange integral J. Their correction is known as the LDA $+ U$ approximation and has been used to self-consistently calculate the NiO density of states by means of the LMTO-ASA method. These authors found a forbidden bandwidth equal in magnitude to the experimental value for converged U- and J-values equal to 8 eV and 0.95 eV respectively. The electronic states sequence corresponds to that of a wide-gap magnetic insulator of the charge-transfer type with the occupied 3d bands below the oxygen 2p bands. Another calculation has been undertaken by Wei and Qi [14]. Their study is distinguished from the former by the spin-polarized approach followed within a discrete variational method applied to a cluster. The latter authors find a gap of 3.7 eV for NiO with U being 6.1 eV, taken from Zaanen and Sawatzky

[15]. The relative positions of the p and d bands are similar to the results of Anisimov *et al* [13] and confer a charge-transfer character to NiO. The LSDA + U method with its additional orbital potential is close in nature to the orbital polarization correction presented by Norman [16]. Both corrections try to reduce the drawbacks resulting from the use of spherical densities which equally populate each d level. Whereas Norman [16] assumes an open-shell correction based on a crystal-field basis, Anisimov *et al* [13] introduce the Coulomb interaction U arising from the fluctuation contributions generally neglected in the mean-field approximation.

The various approximations developed to take into account the correlations yield fairly similar results in the sense that the occupied d bands are contracted and lowered in energy. Most of the recently obtained ground-state densities display an upper p valence band and a d band in the region of the resonant photoemission peak. They support the band picture provided by Fujimori and Minami [2] and consequently the charge-transfer nature of NiO. Nevertheless a different point of view can be maintained when the angular photoemission measurements are considered. Indeed, the recent measurements of Shen *et al* [17] and those of Kuhlenbeck *et al* [18] show a dual band structure. Very dispersive bands appear below flat bands in the Γ–X direction. The broad bands have been assigned to the oxygen functions and the narrow bands to the metal ones. The experimental band organization is in opposition to the current theoretical scheme. This alternative picture can also be supported by reference to the detailed and argued analysis presented by Hüfner *et al* [19].

In contrast to other work dealing with the LSDA + U model [2, 14] our goal is to show that the U-correction is able to derive dispersion curves close to the angular experimental results. This may possibly be realized with a the local density describing at best the real crystal density. In our approach the local density can be adjusted to some extent by means of the procedure described in the next section. A major part is played by the corrective orbital potential which depends on the occupation numbers. The itinerant states are expanded in terms of localized atomic-like orbitals via the LCAO method which accounts well for the localization of the d electrons. The whole derivation is only meaningful if the upper valence band displays significant 2p admixture.

2. Method

The ground-state density is obtained through the self-consistent solution of the Kohn–Sham [5] crystal equation. Each iteration of the self-consistent procedure is divided into two steps. The first step provides a basic set of atomic-like orbitals used to expand the basis Bloch functions. The second step performs the electronic density together with the orbital occupation numbers required to carry out the convergence procedure. At every cycle the crystal wave-function expansion coefficients are calculated for a modified basis set. The degree of convergence is estimated by the deviation between the band charge and the local charge densities.

The localized orbitals proceed from the solution of a one-particle Kohn–Sham equation within the local density approximation (LDA) for each atom of the unit cell. The local one-particle equation reads

$$\left[-\frac{1}{2}\nabla^2 + V^{\alpha}(r)\right]\varphi^{\alpha}_{nl}(r) = \varepsilon^{\alpha}_{nl}\,\varphi^{\alpha}_{nl}(r) \tag{1}$$

where the $\varepsilon^{\alpha}_{nl}$ are the atomic-like eigenvalues for the isolated atom α, and the $\varphi^{\alpha}_{nl}(r)$ represent the corresponding atomic-like radial parts for level n, l.

The space is divided into two regions. Inside a muffin-tin region the potential is the sum of the electron–nucleus, the Coulomb, the exchange–correlation and the intercell potentials:

$$V^{\alpha}(r) = \frac{-Z^{\alpha}}{r} + V^{\alpha}_{\text{Coul}}(r) + V^{\alpha}_{\text{exch}-\text{cor}}(r) + V^{\alpha}_{\text{intercell}}(r). \tag{2}$$

The Coulomb and exchange–correlation potentials are expressed through a so-called one-centre crystal density $\rho^{\alpha}_{\text{crys}}(r)$ attached to each site and defined later in (3). The Coulomb potential is written as

$$V^{\alpha}_{\text{Coul}}(r) = \int \frac{\rho^{\alpha}_{\text{crys}}(r)}{|\boldsymbol{r} - \boldsymbol{r}'|}\, \mathrm{d}r'$$

and is calculated from the spherically averaged electron density in the usual way.

For the exchange–correlation potential we retain only the non-gradient term. Since the study deals with a spin-polarized calculation the parametrized expression given by von Barth and Hedin [20] has been used. The values of the parameters have been taken from Moruzzi *et al* [21].

The potential created by the other cells is the long-range contribution exerted by the ionic charges located on the crystal sites:

$$V^{\alpha}_{\text{intercell}}(r) = \sum_{\beta \neq \alpha} \frac{q_{\beta} e}{\boldsymbol{r} - \boldsymbol{r}_{\beta}}$$

where q_{β} gives the value and the sign of the ionic charge in electron units.

Outside the muffin-tin sphere a constant potential V^0 is assumed. Its role is to compact the tail of the orbitals while keeping the nodes practically in their free-atomic positions. The atomic-like orbitals for the crystal-atom species are calculated self-consistently using a Herman–Skillman [22] program which gives them in tabular form. The numerical basis set is composed of orbitals corresponding to the occupied and lowest-lying unoccupied levels. These localized orbitals serve to form a Bloch basis set for the crystal eigenfunctions and to construct a one-centre atomic-like local density $\rho^{\alpha}_{a}(r)$ expressed as

$$\rho^{\alpha}_{a}(r) = \sum_{n,l}^{oc} P^{\alpha}_{n,l} \left|\varphi^{\alpha}_{n,l}(r)\right|^2. \tag{3}$$

The summation is over all of the occupied orbitals with occupation numbers $P^{\alpha}_{n,l}$. These are fractionary numbers describing the configuration of an atom in its crystal environment.

The crystal potential is the sum of muffin-tin potentials derived from the local densities $\rho^{\alpha}_{a}(r)$ ascribed to each site. The constant potential V^0 introduced in order to obtain a local basis set does not appear in the crystal potential. It is expressed as

$$V_{\text{crys}}(\boldsymbol{r}) = \sum_{\upsilon} \sum_{\alpha} V^{\alpha}(\boldsymbol{r} - \boldsymbol{R}_{\upsilon})$$

where υ designates the crystal unit cells and α the sites within the unit cell.

V^{α} is the potential defined inside the muffin-tin sphere centred on site α according to equation (2) with $\rho^{\alpha}_{a}(r)$ as input.

The crystal eigenstates $\Psi_{\lambda}(\boldsymbol{k}, \boldsymbol{r})$ are developed in terms of Bloch functions $\Phi_{j}(\boldsymbol{k}, \boldsymbol{r})$ in the usual manner:

$$\Psi_{\lambda}(\boldsymbol{k}, \boldsymbol{r}) = \sum_{j} a^{\lambda}_{j}(\boldsymbol{k}) \Phi_{j}(\boldsymbol{k}, \boldsymbol{r})$$

where j stands for the crystal site α and for both of the atomic quantum numbers n and l, and λ indicates the band to which the eigenstates are related.

The ground-state crystal charge density $\rho_{\text{crys}}(\boldsymbol{r})$ is expressed as

$$\rho_{\text{crys}}(\boldsymbol{r}) = e \sum_{k \in \text{BZ}} \sum_{\lambda}^{oc} \Psi_{\lambda}^{+}(\boldsymbol{k}, \boldsymbol{r}) \Psi_{\lambda}(\boldsymbol{k}, \boldsymbol{r}).$$

The summations extend throughout the $\boldsymbol{k}$-vectors belonging to the first Brillouin zone and over the occupied bands.

The crystal charge density $\rho_{\text{crys}}^{\alpha}(\boldsymbol{r})$ attached to a particular site α is easily extracted out of $\rho_{\text{crys}}(\boldsymbol{r})$ with the aid of the intermediate quantity $\rho_{\lambda,ij}(\boldsymbol{r})$. The quantity is constructed for two components of an eigenfunction belonging to the λ-band, and reads

$$\rho_{\lambda,ij}(\boldsymbol{r}) = e \sum_{k} a_i^{\lambda +}(\boldsymbol{k}) a_j^{\lambda}(\boldsymbol{k}) \phi_i^{+}(\boldsymbol{k}, \boldsymbol{r}) \phi_j(\boldsymbol{k}, \boldsymbol{r})$$

with

$$\rho_{\lambda,ij}(\boldsymbol{r}) = \rho_{\lambda,ji}^{+}(\boldsymbol{r})$$

where $\phi_i(\boldsymbol{k}, \boldsymbol{r})$ and $\phi_j(\boldsymbol{k}, \boldsymbol{r})$ are basis Bloch functions expanded in terms of the localized orbitals obtained in the first step.

The $a_i^{\lambda}(\boldsymbol{k})$ are the expansion coefficients of the eigenfunction belonging to the λ-band.

The above quantity makes it possible to define the charge density $\rho_i(\boldsymbol{r})$ associated with a Bloch function $\phi_i(\boldsymbol{k}, \boldsymbol{r})$ through the relation

$$\rho_i(\boldsymbol{r}) = \text{Re}\left[\sum_{j} \sum_{\lambda}^{\text{occup}} \rho_{\lambda,ij}(\boldsymbol{r}) \right].$$

The definition of $\rho_i(\boldsymbol{r})$ implies that we use a Mulliken [23] population partitioning in which the cross terms are divided equally between the relevant sites. Obviously many possibilities of sharing the mixed terms among the sites exist. If another partitioning is adopted it should be mentioned, since the converged results depend on the new prescription. In practice we use a radial charge density in order to solve a one-dimensional Poisson equation for obtaining the muffin-tin potentials entering the crystal potential expression.

The charge density belonging to a crystal site α is the sum over the contributions of all of the occupied orbitals centred on the site. After integration over the longitudinal and azimuthal angles the band charge density $\rho_{\text{crys}}^{\alpha}(\boldsymbol{r})$ is given by the relation

$$\rho_{\text{crys}}^{\alpha}(r) = \sum_{i, \alpha \text{ fixed}} \rho_i(r). \tag{4}$$

The crystal charge density is then cast into the crystal band densities belonging to each site according to the expression

$$\rho_{\text{crys}}(r) = \sum_{\alpha} \rho_{\text{crys}}^{\alpha}(r).$$

The population $P_{n,l}^{\alpha}$ related to the Bloch function $\phi_i(\boldsymbol{k}, \boldsymbol{r})$ is expressed as

$$P_{n,l}^{\alpha} = P_i = \int \rho_i(r) \, \mathrm{d}r.$$

In our procedure the same occupation numbers are assumed for the atomic-like functions $\varphi_{n,l}^{\alpha}(r)$ to be found in expression (3).

The ionic charge Q^{α} on one site α is easily defined via the atomic number Z^{α}:

$$Q^{\alpha} = Z^{\alpha} e - \sum_{i \in \text{site}\, \alpha} P_i.$$

The first cycle of the self-consistent procedure is not performed with an initial guess for the $P^{\alpha}_{n,l}$ but with a local potential expressed as a superposition of free-atomic potentials. The single potential for each constituent of the unit cell is derived from an individual potential corrected by a spherically averaged contribution from the neighbouring atoms as exposed in reference [24]. The self-consistent criterion adopted at present is the stabilization on the population numbers $P^{\alpha}_{n,l}$. At convergence, the crystal eigenfunctions $\Psi_{\lambda}(\boldsymbol{k}, \boldsymbol{r})$ are consistent with the crystal charge density $\rho_{\mathrm{crys}}(r)$ while the atomic-like orbitals $\varphi^{\alpha}_{n,l}(r)$ are consistent with the local atomic density $\rho^{\alpha}_{a}(r)$. The two densities always show a residual density $\Delta\rho^{\alpha}(r)$, so self-consistency cannot be fully achieved:

$$\Delta\rho^{\alpha}(r) = \rho^{\alpha}_{\mathrm{crys}}(r) - \rho^{\alpha}_{a}(r).$$

Our density definitions lead to $\int \Delta\rho^{\alpha}(r)\,\mathrm{d}r = 0$, so the meaningful deviation σ^{α} measuring the quality of convergence is defined as

$$(\sigma^{\alpha})^2 = \frac{1}{\Omega}\int \frac{(\Delta\rho^{\alpha}(r))^2}{4\pi r^2}\,\mathrm{d}r$$

where Ω is the unit-cell volume.

Even if a variational procedure is engaged to minimize the difference, the latter can never vanish since $\rho_{\mathrm{crys}}(r)$ is expressed in terms of delocalized states and $\rho^{\alpha}_{a}(r)$ in terms of localized levels. In fact, σ^{α} falls to small values for localized levels like the d orbitals of nickel and to acceptable values for the oxygen. As a result the simple occupation number convergence scheme makes the Kohn–Sham equation compatible with the atomic-like basis set. The optimal local basis retained here is the one which leads to satisfactory agreement between the calculated and experimental observables.

It is worth mentioning that the constant potential outside the muffin-tin region allows an additional degree of flexibility since it is possible to more or less compress the atomic-like orbitals. This freedom can be used to modify the atomic configuration and the related ionicity of the crystal constituents. Thus the framework of the method is first to choose an atomic-like numerical set related to the localizing potential V^0 and second to make the crystal Kohn–Sham equation consistent with the limited local basis. The degree of self-consistency is estimated by the values of the σ^{α}. The method outlined can be considered as a simplified variant of the discrete variational method presented by Zunger and Freeman [25]. Two main differences are to be noticed: $\Delta\rho^{\alpha}(r)$ is not variationally minimized according to the occupation numbers $P^{\alpha}_{n,l}$ and the densities are only expressed in the radial coordinates.

The LCAO formalism based on the local spin-density approximation (LSDA) has been used to represent the crystal Kohn–Sham equation. The muffin-tin volumes at each atomic site overlap but are limited by the condition that the sum of the volumes must be equal to the volume of the unit cell. The potential overlap is only effective between the first neighbours, in the case of the second neighbours the most stringent condition that we can impose is for them to touch. The general expressions for the diagonal and off-diagonal matrix elements have been derived in [24]. These elements have been developed in a classical manner in terms of overlap, crystal and potential integrals. Only two-centre integrals are taken into account and are calculated by numerical integration from the tabulated potentials and atomic-like functions.

The LSDA + U approximation essentially substitutes for the mean orbital occupation number with its effective occupation. This improvement is achieved by means of a corrective potential $V_{m\sigma}$ proposed by Anisimov *et al* [13]. For a spin-polarized density of states the expression reads

$$V_{m\sigma} = U\sum_{m'}(n_{m'-\sigma} - n_0) + U\sum_{m'\neq m}(n_{m'\sigma} - n_0) - I\sum_{m'\neq m}(n_{m'\sigma} - n^{\sigma}_0).$$

The $V_{m\sigma}$-potential is orbital dependent and operates only on partially occupied shells. It is expressed through the Hubbard interaction U which is at present considered as an adjustable parameter and through the Stoner parameter I which is calculated in each iteration. As a result, the additional potential polarizes the orbitals and generates a non-spherical density for an unfilled d shell. In this sense the correction takes correlation effects into account since the electron trajectories follow their orbital symmetries and depart from the spherical symmetry. A polarized orbital lowers the non-corrected LSDA potential and thus reduces the importance of the electronic Coulomb interaction. The $V_{m\sigma}$-potential is treated as a first-order perturbation in our scheme and acts in each matrix element build-up with the metal d functions.

3. Results

Our results are devoted to a spin-polarized calculation applied to antiferromagnetic NiO. Following the derivation of Slater [3], the majority $\uparrow$ and the minority $\downarrow$ spins are set apart by a specific potential operating on each spin direction. As the exchange correlation potential is stronger for the majority-spin system this latter will be pulled down below that of the minority-spin system. Going from a metal $\uparrow$ to a metal $\downarrow$ the 3d spin directions have to be reversed. But the majority-spin system for both the metal $\uparrow$ and the metal $\downarrow$ sees the same potential and so does the minority-spin system. This explains the double degeneracy of the spin-polarized density of states.

The distinction between the two spin systems has an effect on the space group identification. The electrons with a given spin direction feel a distinct potential as they move from one site to another one. From a crystallographic point of view one simulates this fact by considering two metal species. NiO in its antiferromagnetic phase is to be considered as an ABO_2-type compound which belongs to the rhombohedral D^5_{3d} space group.

The initial atomic configurations used for the definition of the local basis sets are $1s^2 2s^2 2p^6 3s^2 3p^6 3d^8 4s^0 4p^0$ for the nickel ion and $1s^2 2s^2 2p^6$ for the oxygen ion. The secular matrix is spanned by the 2s and 2p oxygen functions together with the 3d, 4s and 4p metal functions. They generate a 26-by-26-dimensional matrix since the magnetic unit cell is twice the paramagnetic unit cell. The chosen radii for the metal and oxygen spheres are respectively 2.65 au and 2.8 au. The convergence of the occupation numbers is considered as achieved once the values of the $P^{\alpha}_{n,l}$ are stable up to five figures. The total number of electrons obtained after adding up all the $P^{\alpha}_{n,l}$ is accurate to within 0.005 of an electron.

The LSDA residual differences between the output ground-state density and the input local density for the metal and oxygen ions are depicted in figure 1. The distortion is negligible for the nickel ion and indicates the adequacy of the ionic configuration and the ground-state crystal density. This is a consequence of the local nature of the d orbitals. The local density is scarcely distorted and simulates the crystal density around the nickel site to a good approximation. The residual $\Delta\rho^{\alpha}(r)$ for the oxygen ion exhibits a greater discrepancy which reflects the particular behaviour of the O^{2-} ion. The 2p oxygen functions are known to be very diffuse since their propensity is to occupy the whole space available. They show a greater variability than the d orbitals and are sensitive to small variations in the ionic configuration.

The σ-values taken over the atomic Wigner–Seitz sphere are $0.01e$ for the nickel and $0.096e$ for the oxygen ions. They should be compared to $0.098e$ given by [25] for the unit cell of diamond composed of two carbon atoms. Our simple convergence scheme based on the Mulliken charge yields a lower σ-value for the nickel atom than for the carbon atom.

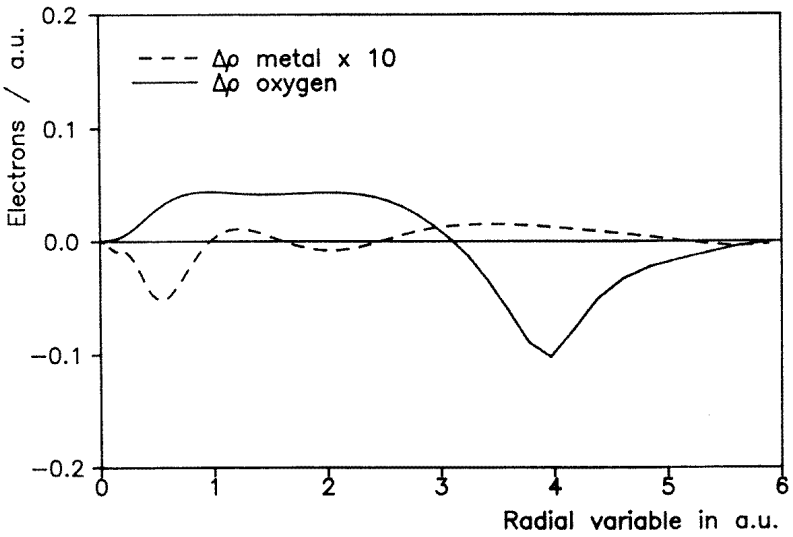

Figure 1. LSDA residual differences in radial coordinates for the metal and oxygen ions.

The result is coherent with the ionic character of NiO since there is no build-up of charge in the interatomic region as in covalent systems. The higher σ-value for the oxygen ion cannot be ascribed to bond formation but rather to a redistribution of the charge around the oxygen. The charge density extends or compresses so as to adapt itself to the volume left by the nickel electronic cloud. The number of displaced electrons can be evaluated as $\frac{1}{2}\int|\Delta\rho^{\alpha}(r)|\ \mathrm{d}r$ and amounts $0.1e$ for the oxygen ion. The σ-values are of the same order of magnitude for the LSDA $+ U$ approximation.

Table 1. The hybridization rate (in per cent) for each band.

	LSDA		LSDA $+ U$	
Bands	2p	3d	2p	3d
2p	91.0	9.0	78.5	21.5
$t_{2g\uparrow}$	4.8	95.2	17.1	82.9
$e_{g\uparrow}$	12.0	88.0	33.4	66.6
$t_{2g\downarrow}$	6.7	93.3	13.2	86.8
$e_{g\downarrow}$	19.8	80.2	8.7	91.3

The self-consistent densities of states are represented in figures 2 and 3 respectively for a simple LSDA and a corrected LSDA$+U$ calculation. When adopting the usual terminology to identify the 3d bands in a cubic field, for the LSDA and with increasing energy order an occupied $t_{2g\uparrow}$ band, an overlapping $e_{g\uparrow}$–$t_{2g\downarrow}$ band and an empty $e_{g\downarrow}$ band are observed. The band gap is between d bands and is of magnitude 0.4 eV. The forbidden gap of 4.1 eV is obtained with a value of U amounting to 5.4 eV together with a Stoner parameter converged to 1.12 eV. The U-correction causes a clear change in the density of states. The unoccupied $e_{g\downarrow}$ band moves towards the 4s band by about 3 eV while the occupied 3d bands are pulled down towards the 2p bands. The 3d bands are not merged into the 2p bands but are spread out into three individual bands since the separation between the $e_{g\uparrow}$ and $t_{2g\downarrow}$ is

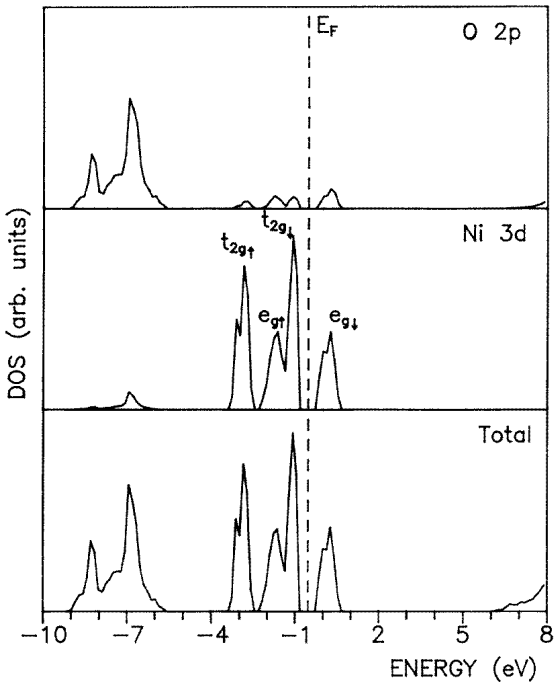

Figure 2. The total and partial ground-state DOS for NiO within the LSDA calculations.

almost achieved. The 2p–3d closeness favours mixing of the orbitals for all of the occupied states. In order to appreciate the importance of the hybridization effect we present in table 1 the p and d contributions within each band. As an example U raises the proportion of the 2p functions in the $e_{g\uparrow}$ band by about twenty per cent but reduces the proportion of the 2p functions in the unoccupied $e_{g\downarrow}$ band by about eleven per cent.

Table 2. Comparison between LSDA and LSDA + U results.

	U (eV)	I (eV)	Ionicity (electrons)	Spin moment (μ_B)	Gap (eV)
LSDA	0	0	1.73	1.61	0.4
LSDA + U	5.4	1.12	1.87	1.91	4.1

Each of the d bands exhibits a modest width, the maximum being 1.25 eV in the case of the $t_{2g\uparrow}$ band. Thus an appropriate basis leads to narrow bands consistent with the description of localized electrons. The ionicity and the magnetic moment are summarized in table 2, where it is noted that the LSDA + U version increases both quantities. The theoretical moments fall into the experimental interval ranging between 1.6 and 1.9 μ_B [26–28]. The best agreement with the experiment is given by the LSDA + U approach and corresponds to the highest moment and ionicity. The ionicity is close to the integer value of two electron charges and corroborates the existence of the O^{2-} ion in NiO. The presence of that ion was suggested earlier when optical experiments were successfully interpreted with the ligand-field model.

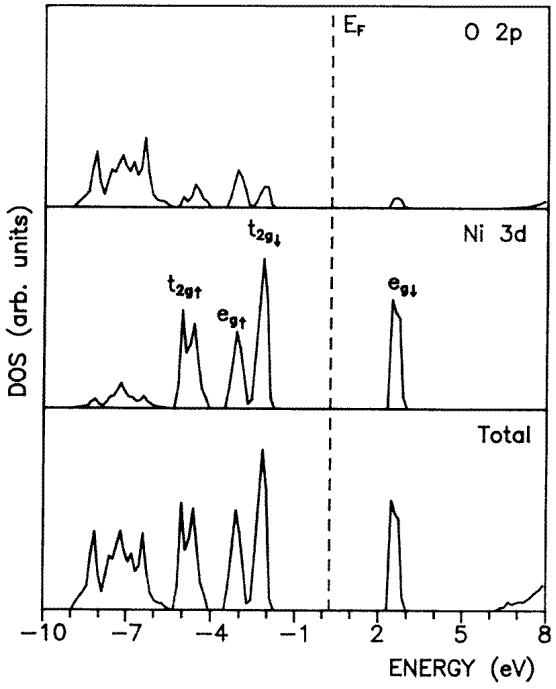

Figure 3. The total and partial ground-state DOS for NiO within the LSDA + U calculations.

4. Discussion

The consequent ionicity, obtained in both the LSDA (1.73e) and the LSDA + U (1.87e) approaches, indicates a strong probability that a doubly ionized oxygen ion is present. The existence of O^{2-} is quite likely in a cubic solid owing to the stabilizing Madelung potential on the anion site. The ionic character basically influences the occupation of the 3d metal orbitals. It is well known that an octahedral environment spreads the d levels into a t_{2g} triplet with xy-, yz- and zx-symmetry below an e_g doublet with $x^2 - y^2$ and $3z^2 - r^2$ symmetry. Further a spin-polarized Hamilonian moves the majority triplet and doublet apart from the minority energy states, the size of the displacement depending on the difference between the majority and minority exchange–correlation potentials. The last three occupied bands together with the first empty band correspond on the energy scale to the $t_{2g\uparrow}$, $e_{g\uparrow}$, $t_{2g\downarrow}$ and $e_{g\downarrow}$ symmetries for the two LSDA and LSDA + U versions. The assignment is the result of the symmetry analysis of the orbitals attached to the electronic states and has been checked by a partial density of states projection. The basis d functions spanning the triplet and doublet subspaces are those pointed out by the ionic model even if the 2p hybridization precludes a perfect distribution. The occupied states taken up to the Fermi level supply integer values for eight d orbitals. Thus the occupation number is exactly one for the five d majority orbitals, as for the minority electrons filling the three xy-, yz- and zx-orbitals. The classical behaviour of the d orbitals in an ionic crystal can be recognized. The preferential occupation of the $t_{2g\downarrow}$ levels has been observed experimentally by Sasaki *et al* [29] on the density lines where a departure from the spherical symmetry becomes clearly visible.

The comparison between our LSDA and the ground-state density of Terakura *et al* [4]

reveals a noticeable difference. A forbidden gap of more than 2 eV spreads the p from the d states in figure 2 whereas the energy levels are continuously distributed up to the Fermi level in [4]. The explanation comes from the additional flexibility introduced by the localizing potential. Besides the possible variation of the potential radii ratio common in the two approaches, a further degree of freedom is ensured by the constant potential. Indeed for each fixed V^0 defining a proper set of atomic-like functions the consistent solution of the Kohn–Sham equation provides a different outcome. In our self-consistent calculations the muffin-tin ratio $R_{\mathrm{Ni}}/R_{\mathrm{Ox}}$ has been fixed to 0.943 (1.13 in [4]) and the localizing potentials to 1.12 au for nickel and 0.13 au for oxygen. This choice gives an ionicity of 1.73e and a magnetic moment amounting 1.6 μ_B. Now the currently calculated LSDA magnetic moments given by several authors are about one μ_B. Such low theoretical values suggest a nickel-to-oxygen charge transfer that we estimate to be around one electron. The degree of charge transfer has a clear effect on the nature of the electronic states subspanning the valence bands. For an ionicity of two electrons, six p- and eight d-type electrons have to be accommodated within the valence band. In contrast, for a one-electron charge transfer the valence states are distributed over five p and nine d symmetry levels. In the latter case the p and the d states are more strongly mixed and give rise to a broadening of the p band. As an example, if V^0 is fixed equal to 1.2 au for the nickel and to 0.5 au for the oxygen, the ionicity reduces to 1.25e and the forbidden p–d gap to 1.3 eV. These findings demonstrate that the results depend on the converged occupation numbers in agreement with the results of [25]. The trend already checked in [4] is that both the magnetic moment and the nickel-to-oxygen charge transfer vary in the same way. According to our results we believe that a significant charge transfer is necessary in order to obtain a magnetic moment close to the recorded experimental values. The high ionicity also provides quite a simple argument for explaining the discrepancies with previously published LSDA works.

The recent theoretical estimations for U show some dispersion. An LDA self-consistent calculation performed by Anisimov *et al* [13] ascribes 8 eV to U. A far more significant value has been given by Towler *et al* [30]. The authors found 28 eV for the Coulomb energy in their Hartree–Fock approximation. Our adopted value of 5.4 eV is of the same order of magnitude as the empirical estimations. Thus from spectroscopic data Brandow [31] deduced 5.8 eV for U, whereas Zaanen and Sawatsky [15], from energetic and screening considerations, value U at 6.1 eV. The disagreement between the theoretical and the empirical values stresses the real difficulty in numerically estimating U for atoms in a solid. The qualitative definition usually admitted is the energy required to put a supplementary electron into a 3d orbital when the electron jumps from one site to another. Assuming no spin flip during the hopping process, U has to be less than or equal to the energy separation between the occupied and the empty $\mathrm{e_g}$ bands. Indeed, a metal $\uparrow$ can receive a ninth electron with spin $\downarrow$ in either one of the unoccupied x^2-y^2 or $3z^2-r^2$ orbitals. This extra electron proceeds from the occupied $\mathrm{e_{g\downarrow}}$ band issued from the metal $\downarrow$ on account of the double degeneracy of the bands. The same reasoning can be used when a supplementary electron is put in a metal $\downarrow$. The present U-value is consistent with the definition since the gap between the $\mathrm{e_{g\uparrow}}$ and $\mathrm{e_{g\downarrow}}$ bands is 5.58 eV.

The value of 5.4 eV ascribed to U has been obtained by adjusting the theoretical LSDA$+U$ gap to the experimental value. According to the derivation of Mattheiss [32] the crystal-field separation can be expressed in terms of a pure ionic and a covalent contribution. For NiO the $\mathrm{t_{2g}}$–$\mathrm{e_g}$ splitting is governed by the covalence term which depends on the overlap between the metal 3d and the surrounding oxygen 2p orbitals. The variability in the 2p spatial extent does not greatly affect the p–d overlap and hopping integrals since the localized 3d functions feel only the tails of the 2p functions. As a consequence the small forbidden

band appearing in the non-corrected LSDA approach is not very sensitive to the choices of $R_{\mathrm{Ni}}/R_{\mathrm{Ox}}$ and V^0. In order to match the theoretical with the experimental gap, the additional U-correction has to enhance the crystal-field effect. This interpretation holds whatever the solutions derived from the variations of the two parameters are. It turns out that the required U-value does not vary over a large energy interval but that it ranges between 5.2 and 6.2 eV.

Table 3. A comparison between recently published fundamental quantities.

	U (eV)	Spin moment (μ_B)	Gap (eV)
LDA + U Anisimov *et al* [13]	8	1.59	3.1
LDA + U Anisimov *et al* [33]		1.7	3.7
LSDA + U Wei and Qi [14]	6.1	1.7	3.7
Hartree–Fock Towler *et al* [30]	28	1.924	13.6
LSDA + U present work	5.4	1.91	4.1

The theoretical approaches used to describe the 3d electrons divide into *ab initio* Hartree–Fock studies and LDA treatments. The Hartree–Fock descriptions treat the correlations within local orbital basis sets while the local density approximations provide additional corrections. The theoretical results are summarized for comparison in table 3. It is readily appreciated that the studies based on the U-corrected LDA present values comparable in magnitude as much for the gap as for the magnetic moment. In contrast both the gap and U have too-large values in the converged Hartree–Fock approximation. The apparent agreement between the LSDA+U results masks fundamental deviations in the band patterns. The first difference concerns the amplitude of the band dispersion. Four 3d minibands appear clearly in the work of Wei and Qi [14] and show bandwidths comparable with ours. In contrast, broad $t_{2g\uparrow}$ and $t_{2g\downarrow}$ bands made up of many peaks describe the d-states repartition obtained by Anisimov *et al* [13]. The unfilled $e_{g\downarrow}$ band is like ours in all of the cases reported. A second difference which has a major implication as regards the interpretation of the experimental work concerns the relative position of the 2p and the 3d bands. In fact NiO refers to a charge-transfer or to a Mott insulator according to the character of the highest occupied band. Our investigations lead to a reverse situation with respect to the other LSDA + U approaches [13, 14]. The flexibility of our treatment is by no means capable of overthrowing the p and d bands. The procedure simply makes it possible to more or less extend the orbital space occupation with the property that an orbital extension on one site is balanced by an orbital contraction on the neighbour site. The behaviour essentially alters the ionicity and the moment and—not so much—the orbital energy levels.

In the following section we would like to make some remarks about the assignments of the experimental bands. Both sets of angular photoemission results [17, 18] depict large dispersive oxygen bands below flat d bands. The obvious fact which comes out of the experiments is that the lowest-energy dispersion curves reproduce beyond all doubt the typical behaviour of 2p bands within an NaCl structure [34]. The experimental bands corresponding to the 2p oxygen functions can be considered as standard 2p bands in a cubic system whose features are well reproduced by the angular photoemission results. That evidence is sustained by a simple LDA calculation [17] developed on a cubic lattice. It is

easily seen that the calculated 2p curves fit well with the experimental data. In contrast the LSDA calculations [17] developed on a rhombohedral lattice show less satisfactory agreement since the theory provides six branches to be compared with a single and a doubly degenerate band. In our view the recorded anomaly finds its origin in the treatment of the antiferromagnetism which consists in admitting that the metal ↑ and ↓ atoms can be considered as belonging to two different chemical species. A lack of symmetry is artificially introduced since the oxygen is no longer sixfold coordinated with identical metal atoms. Its surrounding divides into two distinct groups of three atoms each which breaks the cubic symmetry. As a result the Γ–X direction is no longer a symmetry direction in the reciprocal space and removes the degeneracy of the 2p bands. The situation for the 3d bands is interchanged with respect to the LDA and LSDA. The obtaining of a forbidden d gap is not possible for a cubic lattice as demonstrated by Mattheiss [35] but it appears clearly for a rhombohedral lattice associated with the spin-polarized treatment of the antiferromagnetic order [4]. Thus it seems that the improvement obtained for the metal bands with the LSDA is at the expense of the ligand bands. In order to overcome the discrepancy we suggest using magnetic groups. They preserve the chemical nature of the metal ↑ and ↓ atoms and warrant the cubic environment of the oxygen atoms. The distinction between the two metals is realized by considering an extra coordinate which, for antiferromagnetic NiO, is the direction of the moment.

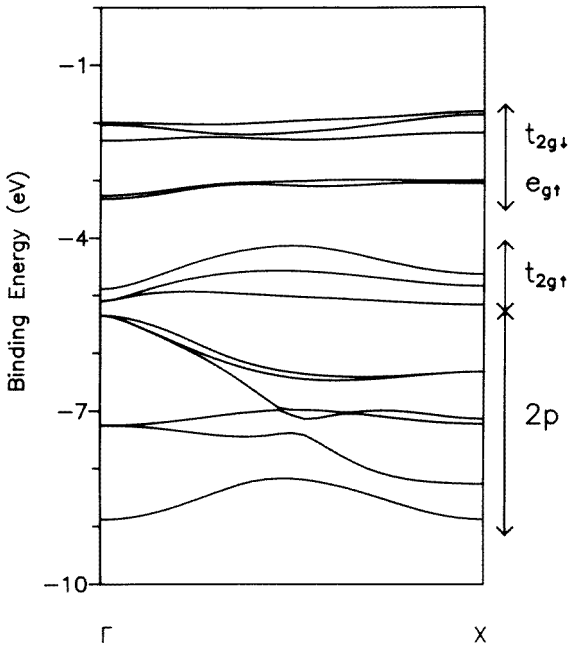

Figure 4. Dispersion curves along the Γ–X direction for the LSDA + U solution.

The theoretical LSDA + U dispersion curves are presented in figure 4. The oxygen 2p bands exhibit the overall experimental width of 4 eV. The $t_{2g\uparrow}$ band is related to the C structure reported in reference [17] and the $e_{g\uparrow}$–$t_{2g\downarrow}$ bands to the A structure. As for the 2p bands, there is also a disagreement about the number of calculated d profiles. The measured A structure contains in fact three dispersion curves [17]—which is still less than the five

predicted branches. A similar observation holds for the C structure since three curves are expected. We believe that, in contrast to the case for 2p bands, the experimental resolution is a possible factor generating the discrepancy, the d levels being very close in energy. If the difference in number between the theoretical and experimental curves is disregarded, our band profiles are similar to the experimental ones both for the character of the bands and for their appearance in energy order. However, the point worth examining is the character of the last occupied band because the 2p admixture within the upper valence band is essential to explain both the spectroscopic results and the existence of the p conduction. The LSDA + U density-of-states projection in figure 3 indicates clear 2p mixing but the part of the 2p contribution at the top of the valence band is not substantial enough to ensure a primarily p character. The remaining question is then that of whether an almost pure p band is needed or whether a mixed p–d band suffices for obtaining quantitative agreement with the experimental data. In the first case the 2p bands lie above the 3d bands and NiO is a genuine charge-transfer insulator. In the second case the 2p and 3d bands are reversed and NiO is instead an altered Mott–Hubbard insulator. The interpretation of the angular photoemission results [17] supported by the present LSDA + U calculations favours the second alternative. The latter energy level order should be adopted only if new developments enhance the ligand contribution to the top filled levels. A 2p rate exceeding fifty per cent would provide a valuable argument in favour of a Mott–Hubbard character of NiO. Let us mention that the present theoretical density agrees with the proposed band scheme of Hüfner *et al* [36] deduced from a coherent interpretation of the available experimental data. Further observations concordant with ours have been reported in the recent work of Aryasetiawan and Gunnarsson [37] where the correlation effects have been introduced via the GW approximation. It appears that the self-energy correction produces the same effects as the U-correction with regard to the reduction of the hybridization in the lowest $e_{g\downarrow}$ conduction band and the 2p mixing in the highest valence band.

5. Conclusion

On one hand the flat dispersion curves lying just below the Fermi level indicate strong evidence for their d character and on the other hand the spectroscopic data are well explained in terms of p holes residing in the upper valence band. These two experimental facts can be reconciled when a strong reduction of the d character at the top of the valence band is assumed. The LSDA + U approach yields results in that direction but the approximation does not give the full answer. Indeed, the prediction of the satellite peak is beyond the possibilities of the one-electron approach. Models describing the whole of the photoemission spectra together with the energy dispersion in k-space would represent appreciable progress.

Acknowledgments

The calculations have been realized thanks to computational facilities granted by the CNI/MAT project 003A94a. The authors are grateful to Mrs W Charles for proofreading the manuscript.

References

[1] Mott N F 1949 *Proc. Phys. Soc.* A **62** 416
[2] Fujimori A and Minami F 1984 *Phys. Rev.* B **30** 957
[3] Slater J C 1951 *Phys. Rev.* **82** 538

[4] Terakura K, Oguchi T, Williams A R and Kübler J 1984 *Phys. Rev.* B **30** 4734
[5] Kohn W and Sham L J 1965 *Phys. Rev.* **140** A1133
[6] Dufek P, Blaha P, Sliwko V and Schwarz K H 1994 *Phys. Rev.* B **49** 10 170
[7] Perdew J P, Chevary J A, Vosko S H, Jackson K A, Pederson M R, Singh D J and Fiolhais C 1992 *Phys. Rev.* B **46** 6671
[8] Dufek P, Blaha P and Schwarz K H 1994 *Phys. Rev.* B **50** 7279
[9] Engel E and Vosko S H 1993 *Phys. Rev.* B **47** 13 164
[10] Vidal J P and Vidal G 1994 private communication
[11] Svane A and Gunnarsson O 1990 *Phys. Rev. Lett.* **65** 1148
[12] Szotek Z, Temmerman W M and Andersen O K 1993 *Phys. Rev.* B **47** 4029
[13] Anisimov V I, Zaanen J and Andersen O K 1991 *Phys. Rev.* B **44** 943
[14] Wei P and Qi Z Q 1994 *Phys. Rev.* B **49** 10 864
[15] Zaanen J and Sawatzky G A 1990 *J. Solid State Chem.* **88** 8
[16] Norman M R 1991 *Phys. Rev.* B **44** 1364
[17] Shen Z X, List R S, Dessau D S, Wells B O, Jepsen O, Arko A J, Barttlet R, Shih C K, Parmigiani F, Huang J C and Lindberg P A P 1991 *Phys. Rev.* B **44** 3604
[18] Kuhlenbeck H, Odörfer G, Jaeger R, Illing G, Menges M, Mull T, Freund H J, Pöhlchen M, Staemmler V, Witzel S, Scharfschwerdt C, Wennemann K, Liedtke T and Neumann M 1991 *Phys. Rev.* B **43** 1969
[19] Hüfner S, Steiner P, Sander I, Neumann M and Witzel S 1991 *Z. Phys.* B **83** 185
[20] von Barth U and Hedin L 1972 *J. Phys. C: Solid State Phys.* **5** 1629
[21] Moruzzi V L, Janak J F and Williams A R 1978 *Calculated Electronic Properties of Metals* (New York: Pergamon)
[22] Herman F and Skillman S 1963 *Atomic Structure Calculations* (Englewood Cliffs, NJ: Prentice-Hall)
[23] Mulliken R S 1955 *J. Chem. Phys.* **23** 1833
[24] Hugel J, Carabatos C, Bassani F and Casula F 1981 *Phys. Rev.* B **24** 5949
[25] Zunger A and Freeman A J 1977 *Phys. Rev.* B **15** 4716
[26] Fender B E F, Jacobson A J and Wegwood F A 1968 *J. Chem. Phys.* **48** 990
[27] Alperin H A 1962 *J. Phys. Soc. Japan Suppl.* B **17** 12
[28] Cheetham A K and Hope D A O 1983 *Phys. Rev.* B **27** 6964
[29] Sasaki S, Fujino K and Takeuchi Y 1979 *Proc. Japan. Acad.* B **55** 43
[30] Towler A D, Allan N L, Harrison N M, Saunders V R, Mackrodt W C and Apra E 1994 *Phys. Rev.* B **50** 5041
[31] Brandow B 1988 *Narrow Band Phenomena* ed J C Fuggle, G A Sawatzky and J W Allen (New York: Plenum) p 97
[32] Mattheiss L F 1970 *Phys. Rev.* B **2** 3918
[33] Anisimov V I, Solovyev I V, Korotin M A, Czyzyk M T and Sawatzky G A 1993 *Phys. Rev.* B **48** 16 929
[34] Pantelides S T 1974 *Phys. Rev.* B **11** 5082
[35] Mattheiss L F 1972 *Phys. Rev.* B **5** 306
[36] Hüfner S, Steiner P, Sander I, Reinert F and Schmitt H 1992 *Z. Phys.* B **86** 207
[37] Aryasetiawan F and Gunnarsson O 1995 *Phys. Rev. Lett.* **74** 3221